Stochastic resonance on two-dimensional arrays of bistable oscillators in a nonlinear optical system

J. P. Sharpe,* N. Sungar, M. Swaney, K. Carrigan, and S. Wheeler
Department of Physics, Cal Poly State University, San Luis Obispo, California 93407
(Received 29 January 2003; published 28 May 2003)

We describe an experimental realization of stochastic resonance in two-dimensional arrays of coupled nonlinear oscillators. The experiment is implemented using an optoelectronic system composed of a liquid crystal light valve in a feedback loop with external, spatially variable noise being added through a liquid crystal display. The behavior of the system differs from previously studied uniform arrays, showing a high signal-to-noise ratio at the output for a broad range of input noise. We show that this behavior is qualitatively the same as that exhibited by computer models where the nonlinear elements of the array have a distribution of biases applied to their switching thresholds.

DOI: 10.1103/PhysRevE.67.056222 PACS number(s): 05.45.Xt

Over the last few decades there has been great interest in the area of noise induced switching in nonlinear systems and especially in stochastic resonance. The latter phenomenon may be defined as the enhanced response of a nonlinear system to subthreshold forcing by the addition of noise. A review of recent work may be found in Refs. [1] and [2].

While earlier work concentrated on single nonlinear elements, more recent interest has been on the effects of coupling the elements together to investigate, for example, noise enhanced propagation and array enhanced stochastic resonance. A thorough computational examination of linear chains of locally coupled nonlinear oscillators has been carried out [3–5] and an extension to two dimensions, where the nonlinear elements are coupled to their four nearest neighbors, was made in Ref. [6]. Other coupling schemes have also been reported [7].

On the experimental side, many investigations have been made of zero-dimensional, or assumed zero-dimensional, systems and Ref. [1] has a good recent overview of these experiments. Studies have also been made of one-dimensional chains of coupled nonlinear diode oscillators [8,9] and Schmitt triggers [10] and these have been shown to exhibit effects such as array enhanced stochastic resonance and noise enhanced propagation.

Here we present an experimental demonstration of stochastic resonance in a two-dimensional system. The experiment is implemented with a liquid crystal light valve (LCLV) in an optical feedback loop to create a bistable response to external inputs. LCLVs have been exploited previously in the context of optical pattern formation and Ref. [11] contains a recent review. Our experimental arrangement is similar to that of Ref. [12] in that we use 1:1 imaging from the output to the input side of the LCLV with the LCLV acting as an amplitude modulator. However, we also have the capability of introducing external, spatially variant noise into the system, as described below.

The LCLV used in this study is a parallel-aligned nematic device from Hamamatsu. The LCLV is composed of thin films of nematic liquid crystal (LC) and an amorphous silicon photodetector sandwiched between two glass plates, which have been coated with transparent conducting layers. An alternating voltage is placed across the thin films and, depending on the quantity of light incident on the photosensor (the ''write'' side of the device), the optically anisotropic molecules in the liquid crystal layer can be reoriented. Light from the other side (the ''read'' side) passes through the LC layer and is reflected back out by a dielectric mirror that isolates this read light from the photosensor. Depending on the orientation of the LC molecules, the phase and polarization state of the reflected light can be modulated. With suitable external optics, this phase or polarization modulation can be converted to an intensity modulation. The Hamamatsu device has a response time of the order of 50 ms and a spatial resolution of about $50\times 50\ \mu\mathrm{m}^2$. The steady state input or output response of the LCLV obtained with a 3-V amplitude, zero offset, 1000-Hz sinusoidal alternating voltage applied across the thin films is shown in Fig. 1 (inset shows the experimental arrangement).

The spatiotemporal response of the LCLV is governed by the following equation [11]:

$$R(r,t) = -\tau \frac{\partial R(r,t)}{\partial t} + l_d^2 \nabla^2 R(r,t) + f(I_{\mathrm{write}}), \qquad (1)$$

where R is the reflectance of the LCLV, r is the two-dimensional spatial coordinate, τ is the relaxation time of the liquid crystal response, and l_d is the transverse diffusion length of the device (arising due to the transverse drift of photoelectrons in the amorphous silicon). I_{write} is the intensity of the light on the write side of the device and the func-

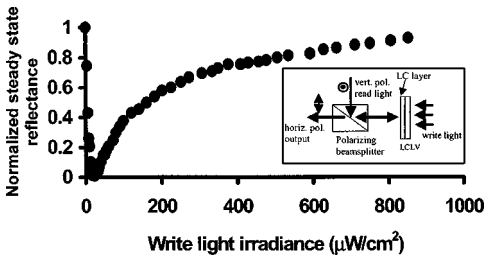

FIG. 1. Input-output relationship for the LCLV with the measurement system indicated in the inset. A spatially uniform light beam ($\lambda = 633$ nm) is incident on the ''write'' side of the device, while vertically polarized light ($\lambda = 633$ nm) is incident on the liquid crystal (''read'') side.

*Corresponding author. Email address: jsharpe@calpoly.edu

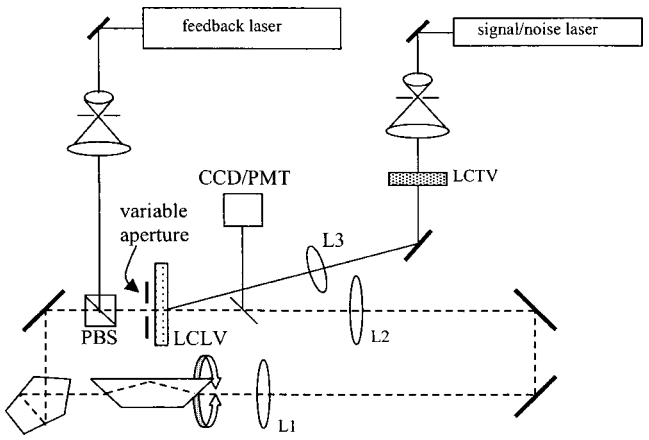

FIG. 2. Experimental arrangement. Spatially filtered, uniform light from the vertically polarized laser ($\lambda = 633$ nm) was incident on the polarizing beam splitter (PBS) and upon reflection from the LCLV imaged 1:1 onto the back side of the LCLV using lenses $L1$ and $L2$ of focal lengths 40 cm. The dove prism was used to remove residual rotations from the feedback loop (indicated with a dashed line) and the penta prism ensured an even number of reflections. The activity in the feedback loop was monitored through a beam splitter using the CCD array and PMT, both conjugate to the LCLV. The LCTV (Kopin Cyberdisplay) was illuminated using a spatially filtered laser beam ($\lambda = 633$ nm) and the display imaged 1:1 on the LCLV using lens $L3$.

tion f is the steady-state (nonlinear) response of the LCLV, shown in Fig. 1. When the LCLV is included in a feedback loop, so that light from the read side of the device is routed back to the write side, then we have $I_{\text{write}} = I_0 R$ where I_0 is the light intensity fed into the feedback loop. Thus I_0 can be used as a control parameter for the system. Equation (1) is the continuous analog of a two-dimensional array of nonlinear, overdamped coupled oscillators [13] with the diffusion length governing the scale of the coupling strength.

The complete experimental arrangement is shown in Fig. 2. Vertically polarized light from the He-Ne feedback laser ($\lambda = 633$ nm) was spatially filtered, collimated, and directed to the liquid crystal side of the LCLV via the polarizing beam splitter. A variable aperture dictated the area of the LCLV that was illuminated and the spatial uniformity of the beam was better than 5% of the average over the aperture. The aperture was placed as close to the LCLV as possible (~ 2 mm) to mitigate the effects of diffraction. This aperture effectively determines the area of the LCLV that can participate in the feedback loop and determines the size of the array. A feedback controlled thermoelectric cooler was found necessary to protect the system against drifts in the ambient temperature and maintained the temperature of the LCLV at $25 \pm 0.1\,^{\circ}\text{C}$.

The deterministic external periodic forcing and the noise were fed into the feedback loop through a Kopin Corporation Cyberdisplay 320 Model 290 monochrome display. This display has 290×218 active pixels on 16-μm centers and exhibits a contrast ratio of $\sim 80{:}1$. Images to be displayed were generated offline as sequences of 32×32 arrays. The image sequences had a sinusoidal modulation of their mean intensity and varying noise was added to each element of the

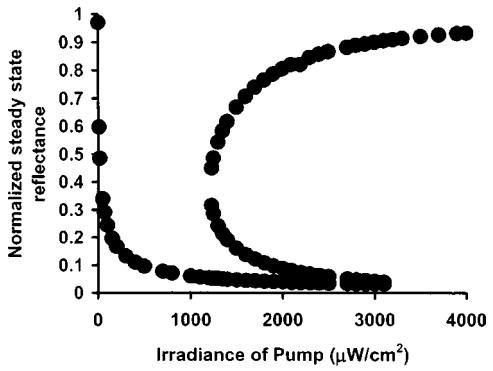

FIG. 3. Bifurcation diagram obtained from analysis of the steady-state response curve of Fig. 1. The ''pump'' is the light sent into the feedback loop (from the feedback laser shown in Fig. 2).

array (hereinafter we will refer to each element of these image arrays as a ''megapixel''). The images were then corrected for the optical response of the display and converted to a 30 frames/sec video signal with a Matrox RT2500 video board that drove the display via a Kopin RS-170 module. The display was imaged 1:1 onto the write side of the LCLV so that each of the megapixels in the image measured $\sim 145 \times 110\ \mu\text{m}^2$. Since the transmission of the display is rather low ($\sim 6\%$ when fully switched on) it was necessary to keep the beam of the illuminating laser narrow to obtain sufficient intensity to switch the LCLV. This meant that the intensity profile of the image of the display on the LCLV was strongly Gaussian [(full width at half maximum) $= 0.2$ cm]—and led to the central area of the LCLV being much more closely biased to switching on than the surrounding areas. The effect of this was to give a nonzero output of the system even with no added noise, as discussed below.

To determine the operating regime of the system we performed an empirical nonlinear fit to the function $f(I_{\text{write}})$, which is plotted in Fig. 1. Using the function obtained from this fit we found the fixed points of the spatially uniform solution of Eq. (1). This yielded the bifurcation diagram of Fig. 3 and showed the existence of two stable fixed points in the region of 1500 $\mu\text{W/cm}^2$ with no added signal (losses in the feedback loop are accounted for in this model). In such an arrangement a bistable response can be obtained so that in the presence of an external signal (from the liquid crystal display) the LCLV can be switched between two stable states (corresponding to bright and dark states). Figure 4 shows the hysteresis curve obtained when we drove the system with a large amplitude, triangularly modulated, 0.5-Hz signal beam.

In order to explore stochastic resonance, the signal beam was adjusted so its average intensity lay between the two stable states (indicated in Fig. 4) and a weak sinusoidal modulation was applied with a peak-to-peak excursion approximately 1/10 of the width of the hysteresis loop. Because of the Gaussian intensity profile of the signal beam it was found that a small patch in the center of the LCLV would be switched on. The sinusoidal frequency was maintained at 0.5 Hz throughout the experiment.

The two-dimensional output from the system was detected using a Cohu 2100 charge-coupled device (CCD) camera, videotaped, and then digitized for analysis. A photo-

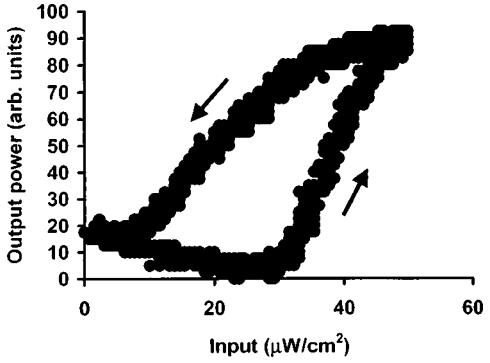

FIG. 4. Hysteresis loop obtained with suprathreshold modulation of a spatially invariant signal beam with no noise.

multiplier tube (PMT) with a 100-μm-diameter pinhole, also conjugate to the LCLV, allowed us to monitor the state of the system in real-time. Time series acquired by the CCD camera were recorded both as a function of the noise intensity and the illuminated area. The area, which was always centered on the same position on the LCLV, was adjusted from $\sim 8\times 10^5$ μm^2 to 2.3×10^6 μm^2, corresponding to a range of megapixels from 50 to 145. The series were analyzed by first thresholding the digitized images between the intensities of the dark and bright stable states and summing the number of bright pixels within the region of the aperture. (In the case where we explored the effects of different array sizes we would only sum the pixels within the area that was determined by the smallest aperture.) We computed the power spectra of the temporal evolution of this signal and calculated the signal-to-noise ratio (SNR) at the frequency of the periodic forcing. Figure 5 shows results with the SNR averaged over a number of different aperture sizes containing from 50–145 megapixels. Two striking features are evident in the results. First, the SNR is relatively flat to a noise level of about 30 dB where it dips and then rises, peaking at $\sim$36-dB noise. Thereafter it falls again at even higher noise, a feature characteristic of stochastic resonance. Second, the variance of the SNR decreases as the noise level is increased. In this experiment we saw no substantial effects of array size on the features of stochastic resonance, which is probably

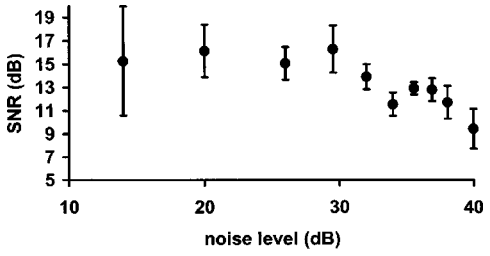

FIG. 5. Signal-to-noise ratio (SNR) of the output from the optical system as a function of noise. These data were obtained using aperture diameters of 1, 1.5, and 1.8 mm with each aperture run with two different noise realizations. In this experiment the SNR was defined as $\mathrm{SNR}=10\log_{10}(p/n)$ where p and n are the power in the signal peak and the average local background, respectively. The noise axis scale is defined as $\mathrm{noise}=10\log_{10}(\sigma^2)$, where σ multiplies a unit variance, zero mean Gaussian process.

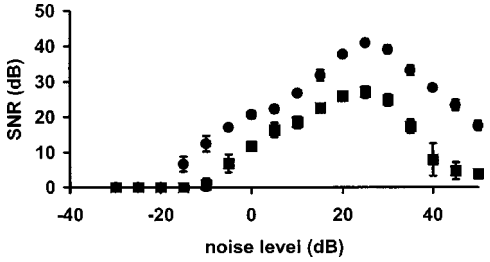

FIG. 6. Comparison of SNRs obtained from an 11×11 array by analyzing the output of the middle oscillator (■) and analyzing the output obtained by summing the number of oscillators in one of the wells at each time step (●). SNR and noise as defined in Fig. 5 caption.

due to the fact that we are already in the plateau regime of the SNR [3,4,6].

We compared the behavior of the experimental system with a computer model of a two-dimensional array of coupled nonlinear oscillators represented by the equation

$$\frac{dx_{m,n}}{dt} = ax_{m,n} - bx_{m,n}^3 + A\sin(\omega t) + \sigma N_{m,n}(t) + \varepsilon(x_{m-1,n} + x_{m+1,n} + x_{m,n-1} + x_{m,n+1} - 4x_{m,n}), \tag{2}$$

where a and b are constants and A and ω are the amplitude and angular frequency, respectively, of the (subthreshold) periodic forcing. σ is a constant that multiplies N, a zero-mean Gaussian noise process, with the noise being local to each element and uncorrelated with the noise at the other elements. ε represents the strength of coupling between the elements. We used the parameters $a=2.1078$, $b=1.4706$, $A=1.3039$, and $f=\omega/2\pi=0.116$ which were introduced in Ref. [3]. We chose to work with Eq. (2) [rather than a direct numerical solution of Eq. (1)] because it would then be possible to assess the changes wrought by varying the parameters of a prototypical bistable system and make direct comparison with previously studied ideal arrays. We obtained output from the computer model by thresholding the output of each individual oscillator and summing the number of oscillators in the right well. In effect, we are counting the number of oscillators in one of the wells at each time step. This procedure was not only the same as that used in the experimental arrangement, but it also avoided problems of phase lag that might be encountered when using other methods such as the occupancy function [3]. We ran simulations on arrays of size 3×3 to 11×11 using 32 cycles of the periodic driving force and starting after the third cycle in order to eliminate transients. The power spectrum of the output signal was obtained and the SNR calculated as described for the experimental results.

We found that characterizing idealized arrays with this method of analysis (as opposed to looking at the output of only the middle oscillator) the shape of the SNR curve was virtually identical to that obtained with the middle oscillator, but increased in magnitude (Fig. 6). This might be expected since we are, in effect, averaging over the oscillators. Our

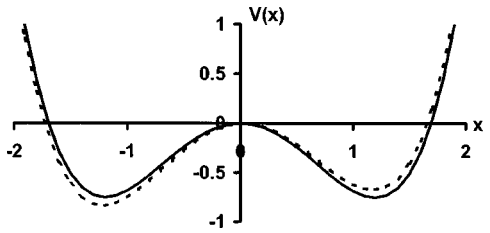

FIG. 7. Potential wells used in the study of biased arrays. The solid line shows the unbiased potential. The potentials are given by $V(x) = -(2.1078/2)x^2 + (1.4706/4)x^4 + cx$, where $c = 0, \pm 0.07$.

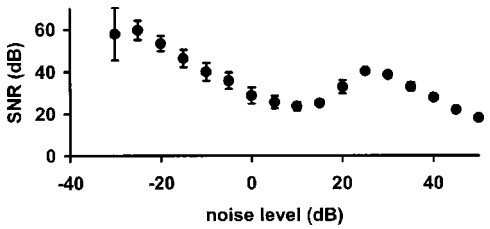

FIG. 8. SNR vs noise for an 11×11 array with a patch of biased oscillators inserted. In this simulation four separate runs, each using a patch of size 2×2, 2×3, 3×3, and 3×4, were inserted in the 11×11 array and the resulting SNRs averaged. The oscillators in the patches had a bias $c = 0.07$ (defined in Fig. 7), were surrounded with a ring of oscillators with zero bias, and the rest of the array had a bias $c = -0.07$. A coupling $\varepsilon = 0.5$ was used. Note that in these simulations the raw output from the oscillator array was thresholded before calculating the SNRs and that it is spatial disorder that leads to high SNR at low noise level, not "intrawell" motion.

computer experiments showed that a distribution in the coupling strengths between the oscillators had very little quantitative impact on the SNRs, as would be expected from earlier studies [3–6].

In the optical experiment we had observed that some regions of the LCLV were turned on even in the absence of noise, which indicates a bias in the bistability or lower thresholds for some regions of the LCLV. In our experiment this arises because the signal beam was strongly Gaussian. In order to study the effect of such regions we simulated two-dimensional (2D) arrays with bias and threshold variations among the oscillators. It was found that introducing a small bias to the wells of the individual oscillators had a major effect on the SNR. In particular, it was found that switching took place even in the absence of added noise and that as the noise increased the SNR fell off to rise again at even higher noise.

In our simulations we inserted a central patch of oscillators with a fixed bias towards one well into a 2D 11×11 array. Around this patch was a ring of oscillators with no bias and beyond that all the other oscillators had a fixed bias towards the other well. Figure 7 shows the potential wells for the biased and unbiased oscillators that were used in the computations. Note that with these biases the uncoupled oscillators cannot switch with the deterministic forcing alone—the oscillators get stuck in one or other of the wells. The SNR peaks that are observed for the case of uniform arrays were always present at the same noise level in the biased arrays, regardless of the distribution in biases we chose.

Figure 8 shows the SNR as a function of noise for the case of a small patch of biased oscillators embedded in an 11×11 array (parameters as shown in Fig. 7 caption). Note that in these simulations the raw output of the array was thresholded before the SNR was calculated. For the low noise levels (<0 dB), where the uniform array has zero SNR, large SNRs were obtained in the biased arrays. In this low noise regime the high SNRs are caused by the switching of oscillators that are at the interface between the two biased areas. In this case the noise does not play a significant role in the switching and is barely present in the output, which explains the high signal-to-noise ratios. In our simulations we checked the actual number of oscillators that are responding to the signal at the lowest noise levels and found it to be from 10–50 % of the total number of oscillators depending on the coupling, biases, and size of the patches. This high SNR behavior at low noise levels disappears for zero coupling and high coupling (such as coupling of 5 for 11×11 arrays). When the input noise is increased more oscillators respond to the signal, but the ratio of the signal to noise in the output decreases. At even higher noise levels (where one finds the optimum SNR in uniform arrays) the SNR rises and peaks at the same position as the uniform array for all distributions of biases and thresholds. At around 20-dB noise the array starts responding to the signal in the same way a uniform array would do, with a peak around 30-dB noise level and then falls off again. The behavior at lower noise levels does not appear to have been previously noted in the literature and is a consequence of the distribution of biases.

In conclusion, we have demonstrated an optical experiment that permits the study of stochastic resonance in coupled nonlinear arrays. The system has been shown to exhibit an unusually broad range of high signal-to-noise ratio as a function of input noise. A simple computer model of coupled oscillators with a range of biases qualitatively captures the behavior of the system. Current work is focused on refining the optical setup, improving computer modeling, and demonstration of nonlinear effects such as noise-enhanced propagation.

J.P.S., M.S., and K.C. would like to thank Research Corporation for support.

[1] L. Gammaitoni, P. Hangi, P. Jung, and F. Marchesoni, Rev. Mod. Phys. **70**, 223 (1998).

[2] *The Constructive Role of Noise in Fluctuation Driven Transport and Stochastic Resonance*, special issue of Chaos **8**(3) (1998).

[3] J. F. Lindner, B. K. Meadows, W. L. Ditto, M. E. Inchiosa, and A. R. Bulsara, Phys. Rev. Lett. **75**, 3 (1995).

[4] J. F. Lindner, B. K. Meadows, W. L. Ditto, M. E. Inchiosa, and A. R. Bulsara, Phys. Rev. E **53**, 2081 (1996).

[5] J. F. Lindner, S. Chandramouli, A. R. Bulsara, M. Locher, and

W. L. Ditto, Phys. Rev. Lett. **81**, 5048 (1998).
[6] N. Sungar, J. P. Sharpe, and S. Weber, Phys. Rev. E **62**, 1413 (2000).
[7] Z. Gao, B. Hu, and G. Hu, Phys. Rev. E **65**, 016209 (2002).
[8] M. Löcher, G. A. Johnson, and E. R. Hunt, Phys. Rev. Lett. **77**, 4698 (1996).
[9] M. Löcher *et al.*, Chaos **8**, 604 (1998).
[10] A. C. H. Rowe and P. Etchegoin, Phys. Rev. E **64**, 031106 (2001).
[11] F. T. Arrechi *et al.*, J. Nonlinear Opt. Phys. Mater. **9**, 183 (2000).
[12] P. L. Ramazza, S. Ducci, and F. T. Arrechi, Phys. Rev. Lett. **81**, 4128 (1998).
[13] B. von Haeften, R. Deza, and H. S. Wio, Phys. Rev. Lett. **84**, 404 (2000).